Scientific Research Publishing

Open Journal of Applied Sciences, 2024, 14, 2943-2954
https://www.scirp.org/journal/ojapps
ISSN Online: 2165-3925
ISSN Print: 2165-3917

Characterization and Modeling of Reinforced Earth Structures

Tchamiè David Midikizi[1*], Oustasse Abdoulaye Sall[1], Déthié Sarr[2], Cheikh Ibrahima Tine[1], Ndeye Seynabou Ndiaye[1], Makhaly Ba[2]

[1]Department of Civil Engineering, UFR SI-University of Thiès, Thiès, Senegal
[2]Department of Geotechnics, UFR SI-University of Thiès, Thiès, Senegal
Email: *tdavid.midikizi@univ-thies.sn

How to cite this paper: Midikizi, T.D., Sall, O.A., Sarr, D., Tine, C.I., Ndiaye, N.S. and Ba, M. (2024) Characterization and Modeling of Reinforced Earth Structures. *Open Journal of Applied Sciences*, **14**, 2943-2954.
https://doi.org/10.4236/ojapps.2024.1410192

Received: September 8, 2024
Accepted: October 25, 2024
Published: October 28, 2024

Abstract

The aim of this study is to characterize soil/reinforcement interaction in reinforced earth structures. The study showed that the internal behavior of this type of structure depends on a number of factors, including the engineering backfill, the reinforcement and the soil/reinforcement interaction. The study also showed that the soil-reinforcement interaction phenomenon is a fairly complex mechanism that depends on the applied load, the geometry of the structure, the characteristics of the soil and a set of parameters characterizing the nailing: density, number and length of reinforcements, inclination of the reinforcements in relation to the sliding surface, mechanical characteristics of the reinforcements and, in particular, the relative stiffness of the reinforcements and the soil. The results showed that the tensile forces developed in the reinforcement are not entirely reversible, and that the soil at the interface undergoes permanent deformation, leading to the appearance of irreversible tensile forces in the reinforcement.

Keywords

Reinforced Earth Structures, Modeling, Earth/Reinforcement Interaction

1. Introduction

Reinforced earth is a construction method based on the combination of compacted earth and reinforcement (metal or synthetic) bonded to a facing (Figure 1). Alternating layers of powdered backfill and horizontally distributed strips of reinforcement lead to the development of interacting forces (Figure 2), giving rise to a fully-fledged composite material capable of resisting its own weight and the actions applied to it throughout the service life of the structure. Analysis of the in-service behavior of reinforced earth structures is based on model studies, full-scale

experiments, laboratory tests (extraction test, direct shear) and numerical calculations. This analysis is generally focused on defining new modelling or design parameters due to the use of new reinforcement elements, new cladding panels, etc. [1]-[4]. Analytical studies are limited to defining new anchorage models for new types of reinforcement [4]-[10]. In the context of studies carried out on structures reinforced with metal reinforcement, we propose to characterize and model them. To do this, we will first establish a behavioral model of the various parts of the structure, with a view to numerical modeling that will enable parametric analysis of the various characteristics of the materials involved. This phase involves establishing mathematical and computer models to simulate the influence of soil properties (weight by volume, angle of friction, reinforcement characteristics (length, density, spacing, etc.). Finally, we analyze and discuss the results obtained. This analysis will enable us to understand the operation of these structures based on the theory of earth thrust and local equilibrium. To analyze the stability of the reinforced earth mass, the screen will be modeled as a web embedded at its base, connected to reinforcement and subjected to the pressure of the embankment. The aim of this study is to analyze the influence of certain parameters on the behavior of reinforced earth walls. The analysis concerns the parameters of the soil/reinforcement interface, the parameters of the reinforced soil, the use of new synthetic reinforcement, the height of the wall and the soil behavior model.

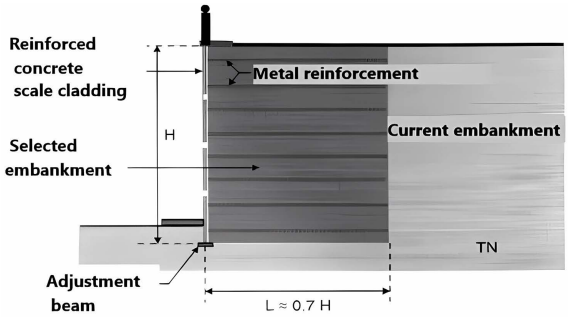

Figure 1. Geometry and components of reinforced earth walls [11].

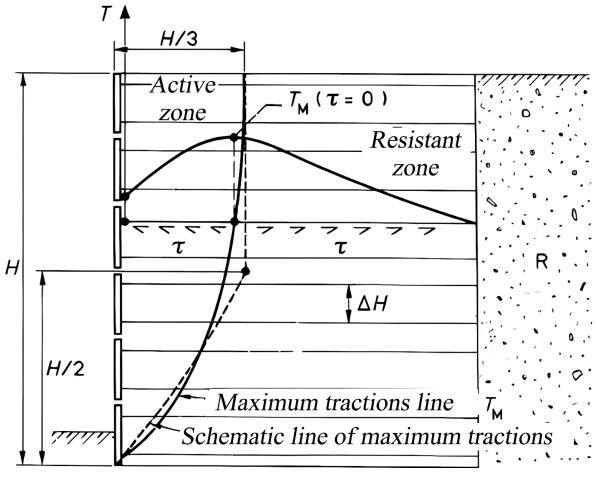

Figure 2. Mobilization of tensile forces in reinforcement [12].

2. Modeling Reinforced Earth Structures

Reinforced earth is a material resulting from the combination of embankment and metal reinforcement in the form of strips, generally of galvanized steel. When the reinforced-earth structure is subjected to stress, the reinforcement is put in tension by friction, giving the soil an anisotropic cohesion. **Figure 1** and **Figure 2** show the geometry and arrangement of reinforcement in a reinforced earth wall, and the principle of stress mobilization.

Around the 1970s, authors began to take an interest in the numerical modelling of reinforced earth structures [13] [14]. Since then, several analytical and numerical calculation methods have been developed to analyze the behavior of these structures and the influence of each element and their parameters [15]-[22]. Analytical and numerical methods are increasingly used to analyze the influence of different material parameters on the stability and behavior of reinforced earth structures.

2.1. External Analysis

External stability is treated in the same way as any other retaining wall stability (e.g. weight wall). Earth pressure is calculated on the fictitious screen parallel to the facing, located behind the reinforcement. Justification is based on punching and sliding at the base of the wall on the foundation soil, as well as block overturning. The results of experimental and numerical studies [23]-[26] have shown that, in the case of metal reinforcements, a reinforced earth wall behaves as a coherent, flexible mass and can admit differential settlements without irreversible disorder. The reinforced earth wall transmits quasi-linear stresses to the foundation soil, due to its own weight (W) and the effects of surcharges and lateral thrusts. The reference stress applied to the base, called σ_v (**Figure 3**), is calculated using the Meyerhof formula in standard NF P 94-270-2009.

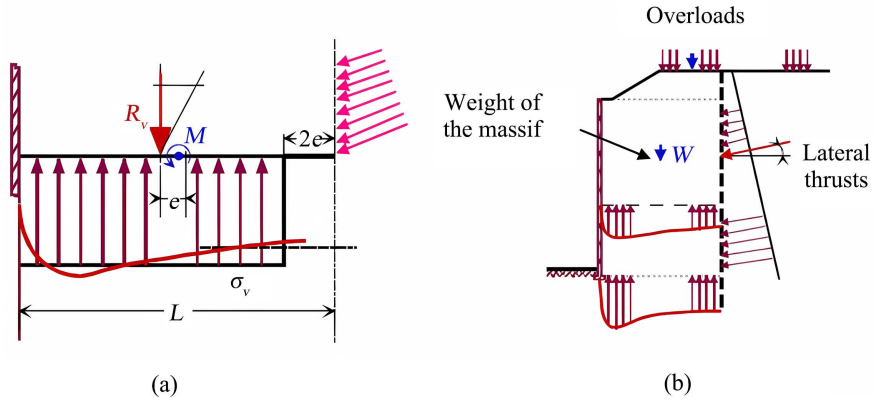

Figure 3. Stress distribution in the foundation soil of a reinforced earth wall [27]. (a) Reference stress; (b) Different types of solicitations.

The reference stress and the value of eccentricity (e) are given by the following relationships:

$$\sigma_v = \frac{R_v}{L - 2e} \tag{1}$$

$$e = \frac{M}{R_v} \tag{2}$$

With:

R_v: vertical resultant per longitudinal meter of facing at the center of the base of the massif;

L: length of the wall corresponding to the length of the reinforcement.

The resulting moment M at the center of the wall base per meter of facing is given by the following equation:

$$M = M_{stab} - M_{renv} \tag{3}$$

$$M = \left[\sum T_{pi}\left(H - zi\right) + M_m + M_q\right] - \left[ka\gamma\left(\frac{H^3}{6}\right) - qKa\left(\frac{H^2}{2}\right)\right] \tag{4}$$

$$M_m = \gamma_m HL/2 \tag{5}$$

$$M_q = qL^2/2 \tag{6}$$

T_p: Maximum tensile stress in each reinforcement bed at the facing;

H: Wall height;

Zi: Depth of reinforcement bed considered;

Ka: Thrust coefficient.

2.2. Characterization of Internal Analysis

Internal stability is verified at the level of each reinforcement bed; the tensile stresses generated in the reinforcement must be less than the soil/reinforcement interface friction resistance and the tensile strength of the reinforcement. Analysis of the internal behavior and distribution of tensile stresses along the metal reinforcement in a reinforced-earth structure has shown that a maximum tensile stress TM is measured at one point of the reinforcement. This point is far from the facing at the top of the wall and close to the facing at depth (Figure 4). All the points form a curve, known as the line of maximum tension, separating the wall into two zones:

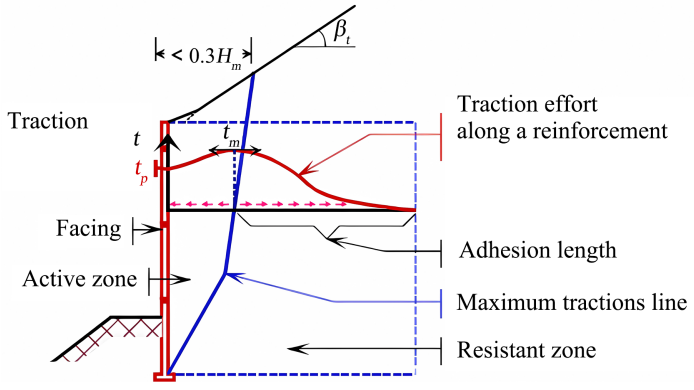

Figure 4. Distribution of tension in the reinforcement of a reinforced earth wall [27].

- The active zone closes to the facing in which the tangential (shear) stress τ exerted by the soil on each face of the reinforcement is directed towards the facing.
- The resistant zone in which the tangential stress τ is directed inwards and the soil tends to retain the reinforcement.

The tangential stress exerted by the soil is given by the following relationship:

$$\tau = \frac{\mathrm{d}T}{\mathrm{d}L}\frac{1}{2b} \tag{7}$$

With:

b: reinforcement width;

L: abscissa on armature;

T: tensile stress in the reinforcement.

2.2.1. Characterization of Tensile Stress T_m

The maximum tensile stress in each reinforcement bed per linear meter of facing is equal:

$$T_m = \sigma_h \cdot S_v \tag{8}$$

where S_v is the vertical spacing between reinforcement beds and σ_h the horizontal stress in the reinforced embankment on a reinforcement bed at the intersection of the maximum tension line.

$$\sigma_h = K \cdot \sigma_v \tag{9}$$

With σ_v the vertical stress determined by Meyerhof's method and K the earth pressure coefficient internal to the mass. In the case of metal reinforcement, in accordance with French standard NF P 94-220:

$$K(z) = K_a\left[1.6\left(1-\frac{z}{z_0}\right)+\frac{z}{z_0}\right] \quad \text{for} \quad z < z_0 \tag{10}$$

$$K(z) = K_a \quad \text{for} \quad z \geq z_0 \tag{11}$$

With $z_0 = 6\,\mathrm{m}$ and K_a the active thrust coefficient equal to:

$$K_a = \tan^2\left(\frac{\pi}{4}-\frac{\Phi}{2}\right) \tag{12}$$

2.2.2. Characterization of Facing Force T_p

The tensile stress in each reinforcement bed at the T_p facing is calculated as follows:

$$T_p = K \cdot \alpha_i \cdot \sigma_v \cdot S_v \tag{13}$$

α_i varies according to the flexibility of the facing. For reinforced earth walls with reinforced concrete scales (**Figure 5**).

3. Modeling Mobilizable Friction in Reinforcement Beds r_f

The mobilizable friction force rf per meter of facing in the reinforcement bed is calculated according to the formula:

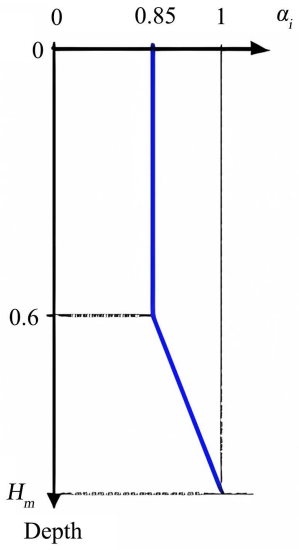

Figure 5. Variation of α_i with depth (case of reinforced concrete scales).

$$r_f = 2 \cdot N \cdot bL_a f^*_{(z)} \sigma_v \tag{14}$$

With:

N: number of reinforcements per meter of facing;

b: frame width;

L_a: length of adhesion in the resistant zone;

σ_v: average value of the vertical stress on the reinforcement bed;

f^*: apparent coefficient of friction at the level under consideration.

The f^* parameter is very important in the design and dimensioning of reinforced earth walls. It characterizes the frictional resistance along the reinforcement, considering soil expansion. The actual friction along the reinforcement is defined by the maximum friction coefficient *f*, which is equal to:

$$f = \frac{\tau_{\max}}{\sigma_v} \tag{15}$$

where σ_v is the average vertical stress applied to the reinforcement and $\tau_{\max}$ the maximum shear stress exerted along the reinforcement. $\tau_{\max}$ can be determined by the maximum tensile stress ($T_{\max}$) in a pull-out test. The maximum tensile stress is reached when the friction is fully mobilized along the reinforcement of length *L*:

$$\tau_{\max} = \frac{T_{\max}}{2bL} \tag{16}$$

In a dense granular soil, under the effect of the shear stresses τ exerted by the inclusion, the soil zone surrounding the inclusion tends to increase in volume, counteracted by the low compressibility of the surrounding mass. $\Delta\sigma_v$ of the initial normal stress σ_{v0} exerted on the surface of the inclusion (**Figure 6**; [12] [28]). So the vertical stress σ_v applied to the inclusion becomes $\sigma_v = \sigma_{v0} + \Delta\sigma_v$. This phenomenon is known as prevented expansion.

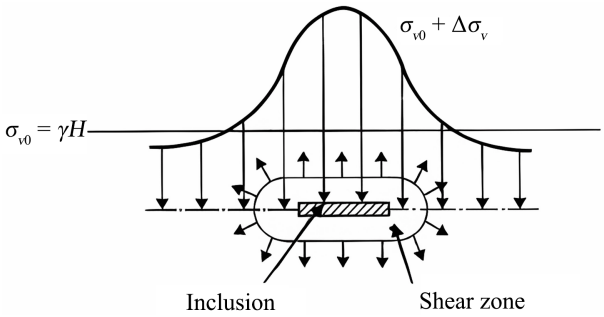

Figure 6. Prevented expansion.

The actual coefficient of friction f is therefore expressed as:

$$f = \frac{\tau_{\max}}{\sigma_{v0} + \Delta\sigma_v} \tag{17}$$

The three-dimensional nature of this phenomenon and the influence of expansion are difficult to consider in dimensioning methods. The increase ($\Delta\sigma_v$) in normal stress (σ_{v0}) is difficult to calculate or predict, and is linked to several parameters (volume of the shear zone surrounding the inclusion, initial normal stresses, compression and soil expansion). [28] defined an apparent friction coefficient f^* to take account of this phenomenon in practice:

$$f^* = \frac{\tau_{\max}}{\sigma_{v0}} \tag{18}$$

This apparent coefficient (f^*) is higher than the real coefficient of friction f and often exceeds 1 in granular soils. It can reach 10 in highly dilatant soils. It depends on the weight of the soil above the reinforcement and its surface condition (**Figure 7**). The increase in the coefficient of friction due to the effect of inhibited expansion is only significant in the case of low vertical stresses. In the case of high vertical stresses, soil dilatancy is negligible. The apparent friction coefficient f^* decreases with increasing confining stress. It varies between f_0^* on the surface of the reinforced mass and f_1^* corresponding to a confinement stress of 120 kPa (**Figure 7**, NF P 94-270).

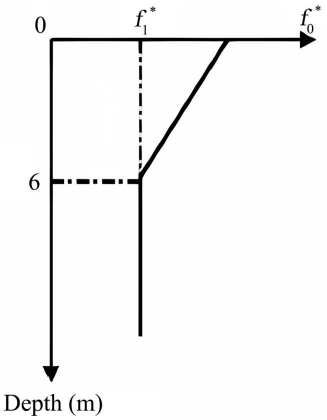

Figure 7. Variation of the f^* coefficient in a reinforced soil mass (NF P 94-270).

4. Results and Discussion

In order to study the interaction between soil and certain types of reinforcement used in the reinforcement of reinforced earth walls, and to highlight the influence of certain parameters (angle of friction, volume weight of backfill, etc.), calculations were carried out on an example structure, with the aim of determining their impact on the maximum tensile and tensile forces at the facing, and on the resulting moment. For the purposes of parametric analysis, the reinforced earth wall studied is a 1 m long slab, with a mechanical height of $H = 7$ m and wall thickness 0.3 m. Figures 8-14 show, respectively, the evolution of tensile forces (T_P and T_m) and resultant moment (M) as a function of height (Z), angle of internal friction φ, embankment weight and vertical spacing S_v.

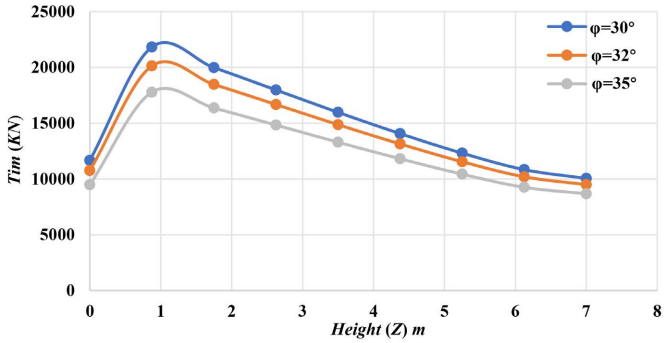

Figure 8. Variation in tensile force at the intersection with the line of maximum tension.

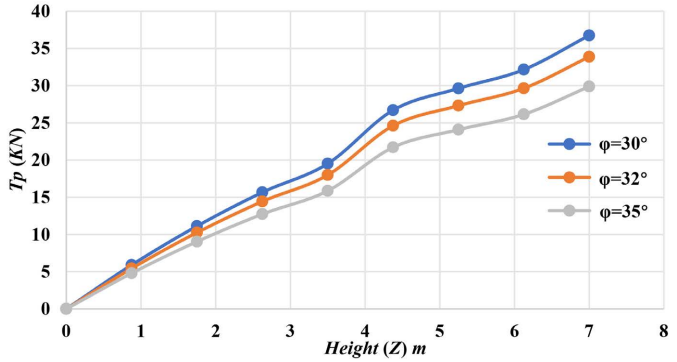

Figure 9. Variation in tensile stress at the facing.

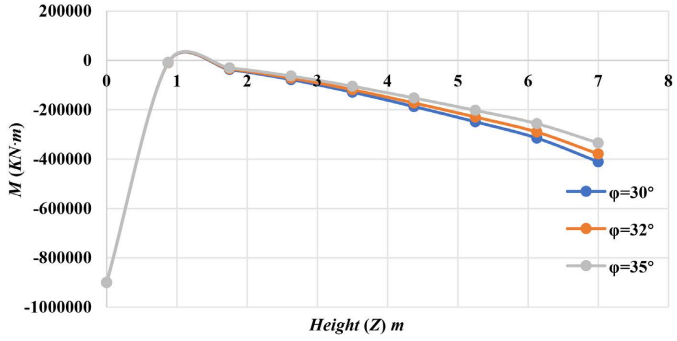

Figure 10. Variation in resultant moment.

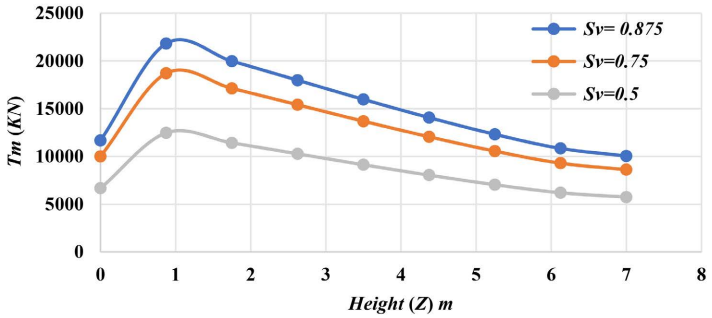

Figure 11. Influence of vertical spacing variation on maximum tensile force.

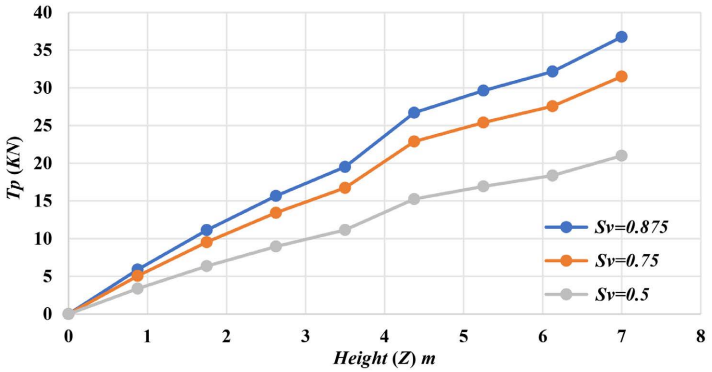

Figure 12. Influence of vertical spacing variation on tensile strength of the facing.

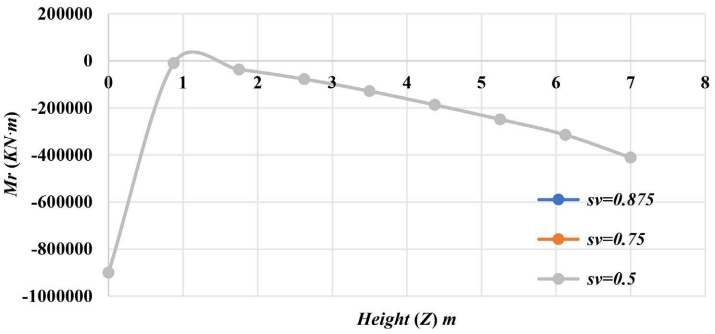

Figure 13. Influence of vertical spacing variation on resultant moment.

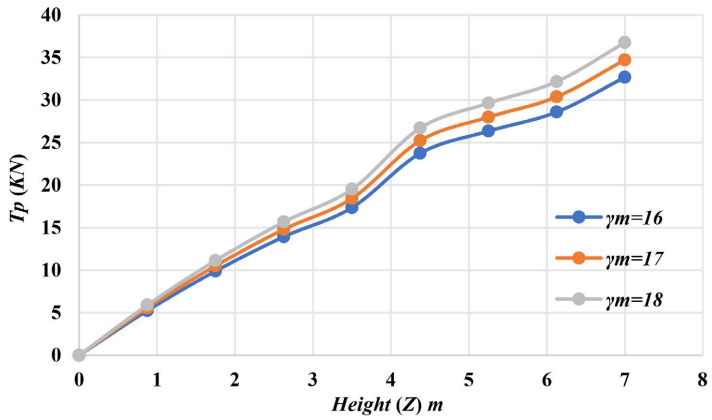

Figure 14. Variation in material weight on facing tension.

Figure 8 and Figure 9 show that the highest tensile stress values were obtained when the value of φ was low. In contrast to the resultant moment, for which significant values were obtained with an φ value. Figure 8 shows that tensile stress (T_m) undergoes three phases in its variation. An increasing trend between 0 and 1 m and a decrease from this value, which represents an extremum. These results show that more the angle of friction is low, more the tensile stress at the facing is great. It can also be seen that this tensile force is less sensitive to the angle of friction at the head and base. Figure 9 shows that the tensile stress T_p at the facing increases with depth and decreases with friction angle. The results in Figure 10 show an increase in the resulting moment between 0 and 1 and a decrease beyond that. These results also show a slight increase in moment with increasing friction. On the other hand, the tensile stress at the facing shows a generally increasing trend, unlike the other stresses. For the first two figures, tensile values are only high if the friction angle is low. This is due to the fact that their expression depends on the thrust coefficient K, which becomes high if φ is low, K becomes high, thus affecting the tensile values. Figure 11 and Figure 12 show that tensile forces are very sensitive to the vertical spacing of reinforcements. These results show an increase in tensile forces with increasing spacing. On the other hand, the resulting moment (Figure 13) is insensitive to vertical spacing. The results in Figure 14 show an increase in tensile stress T_p with the weight of the backfill. We also note that, due to the interaction between the soil and the reinforcement, the tractions developed in the latter are not entirely reversible. In fact, the soil at the interface undergoes permanent deformation, resulting in irreversible tension in the reinforcement.

5. Conclusion

In all cases, the justification of engineering structures requires a soil investigation to determine their mechanical characteristics. In addition, accurate numerical modeling of reinforced earth structures will provide a better understanding of their behavior. Accurate modeling of the entire structure requires, first and foremost, correct and realistic local modeling of the behavior of a reinforcement anchored in the ground. Local modeling of the reinforcement requires the determination of actual interaction parameters at the soil/reinforcement interface. The mechanism of soil-reinforcement interaction is a fairly complex one, depending on the applied load, the geometry of the structure, the characteristics of the soil and a set of parameters characterizing the nailing: density, number and length of reinforcements, inclination of the reinforcements in relation to the sliding surface, mechanical characteristics of the reinforcements and, in particular, the relative stiffness of the reinforcements and the soil. The results show that the behavior of the structure is strongly influenced by soil-reinforcement interaction. The parametric study of soil-reinforcement interaction has enabled us to understand the behavior of the structure under the influence of certain mechanical and geometric characteristics.

Conflicts of Interest

The authors declare no conflicts of interest regarding the publication of this paper.

References

[1] Won, M. and Kim, Y. (2007) Internal Deformation Behavior of Geosynthetic-Reinforced Soil Walls. *Geotextiles and Geomembranes*, **25**, 10-22. https://doi.org/10.1016/j.geotexmem.2006.10.001

[2] Yoo, C. and Kim, S. (2008) Performance of a Two-Tier Geosynthetic Reinforced Segmental Retaining Wall under a Surcharge Load: Full-Scale Load Test and 3D Finite Element Analysis. *Geotextiles and Geomembranes*, **26**, 460-472. https://doi.org/10.1016/j.geotexmem.2008.05.008

[3] Leshchinsky, D. (2009) On Global Equilibrium in Design of Geosynthetic Reinforced Walls. *Journal of Geotechnical and Geoenvironmental Engineering*, **135**, 309-315. https://doi.org/10.1061/(asce)1090-0241(2009)135:3(309)

[4] Abdelouhab, A., Dias, D. and Freitag, N. (2010) Physical and Analytical Modelling of Geosynthetic Strip Pull-Out Behaviour. *Geotextiles and Geomembranes*, **28**, 44-53. https://doi.org/10.1016/j.geotexmem.2009.09.018

[5] Bourdeau, Y., Kastner, R., Bollo-Kamara, N. and Bahloul, F. (1990) Anchoring Behavior of a Geosynthetic Buried in a Two-Dimensional Material. 5*th Franco-Polish Colloquium on Applied Soil Mechanics*, Warsaw, 4-7 September 1990.

[6] Ling, H.I., Wu, J.T.H. and Tatsuoka, F. (1992) Short-Term Strength and Deformation Characteristics of Geotextiles under Typical Operational Conditions. *Geotextiles and Geomembranes*, **11**, 185-219. https://doi.org/10.1016/0266-1144(92)90043-a

[7] Sobhi, S. and Wu, J.T.H. (1996) An Interface Pullout Formula for Extensible Sheet Reinforcement. *Geosynthetics International*, **3**, 565-582. https://doi.org/10.1680/gein.3.0075

[8] Dias, A.C. (2003) Numerical Analyses of Soil-Geosynthetic Interaction in Pull-Out Tests. M.Sc. Thesis, University of Brasilia, 115 p.

[9] Gurung, N., Iwao, Y. and Madhav, M.R. (1999) Pullout Test Model for Extensible Reinforcement. *International Journal for Numerical and Analytical Methods in Geomechanics*, **23**, 1337-1348. https://doi.org/10.1002/(sici)1096-9853(199910)23:12<1337::aid-nag35>3.0.co;2-h

[10] Koerner, R.M. and Soong, T. (2001) Geosynthetic Reinforced Segmental Retaining Walls. *Geotextiles and Geomembranes*, **19**, 359-386. https://doi.org/10.1016/s0266-1144(01)00012-7

[11] Bouafia, A. (2018) Introduction à la réglementation géotechnique, Tome 1, fondations superficielles et profonfes, Département de Génie Civil-Faculté de Technologie Université Saâd Dahleb de Blida, office des publications universitaires 1, Place centrale Ben-Aknoun (Alger).

[12] Schlosser, F. and Guilloux, A. (1981) Le frottement dans le renforcement des sols. *Revue Française de Géotechnique*, **16**, 65-77. https://doi.org/10.1051/geotech/1981016065

[13] Corté, J.F. (1977) The Finite Element Method Applied to Reinforced Earth Structures. *Bulletin de liaison du Laboratoire des Ponts et Chaussées*, No. 90, 37.

[14] Chang, J.C. and Forsyth, R.A. (1977) Finite Element Analysis of Reinforced Earth Wall. *Journal of the Geotechnical Engineering Division*, **103**, 711-724. https://doi.org/10.1061/ajgeb6.0000450

[15] Shafiee, S. (1986) Simulation numérique du comportement des sols cloues; interaction sol-renforcement et comportement de l'ouvrage, Paris.

[16] SETRA (1994) Services d'Etudes Techniques des Routes et Autoroutes, les ouvrages en terre armée, Avenue Aristide Briand.

[17] Dhouib, A. (1994) Behavior and Design of Reinforced Earth Structures under Dynamic Action, Division Leclerc.

[18] Schlosser, F., Jacobsen, H.M. and Juran, I. (1995) Soil Reinforcement.

[19] Soyez, L. and Bourgeois, E. (2009) Étude du comportement d'un mur en Terre Armée: Rôle de l'interface sol/armature dans la modélisation. *Revue Française de Géotechnique*, No. 129, 21-33. https://doi.org/10.1051/geotech/2009129021

[20] Abdelouhab, A. (2010) Behavior of Reinforced Earth Walls. Physical, Analytical and Numerical Modeling of Extensible Reinforcements. Laboratoire de Génie Civil et de l'Ingénierie Environnementale (LGCIE).

[21] Belabed, L., Yahiaoui, J. and Benyaghal, H. (2013) Mechanical Behavior of Reinforced Earth Retaining Walls, Cachan.

[22] Payeur, J.B. (2015) Modélisation du comportement d'un remblai renforcé sous chargement ferroviaire de type TGV, NAVIER Laboratory—Geotechnical Team (CERMES).

[23] Ling, H.I., Leshchinsky, D. and Tatsuoka, F. (2003) Reinforced Soil Engineering: Advances in Research and Practice. Marcel Dekker, Inc.

[24] Yoo, C. and Song, A.R. (2006) Effect of Foundation Yielding on Performance of Two-Tier Geosynthetic-Reinforced Segmental Retaining Walls: A Numerical Investigation. *Geosynthetics International*, **13**, 181-194. https://doi.org/10.1680/gein.2006.13.5.181

[25] Huang, B., Bathurst, R.J. and Hatami, K. (2009) Numerical Study of Reinforced Soil Segmental Walls Using Three Different Constitutive Soil Models. *Journal of Geotechnical and Geoenvironmental Engineering*, **135**, 1486-1498. https://doi.org/10.1061/(asce)gt.1943-5606.0000092

[26] Ling, H.I. and Liu, H. (2009) Deformation Analysis of Reinforced Soil Retaining Walls—Simplistic versus Sophisticated Finite Element Analyses. *Acta Geotechnica*, **4**, 203-213. https://doi.org/10.1007/s11440-009-0091-6

[27] Flarbi Chaht, F. and Louhibi, Z. (2013) Conception et modelisation d'un ouvrage en terre armee (approache geotechnique). 2*eme Séminaire International sur l'Industrie Minérale et l'Environnement*, Annaba, 19-20 November 2013, 6 p.

[28] Schlosser, F. and Elias, V. (1978) Friction in Reinforced Earth. *Proceedings of the ASCE Symposium on Earth Reinforcement*, Pittsburgh, April 1978, 735-764.